

# Mechanics unlocks the morphogenetic puzzle of interlocking bivalved shells

Derek E. Moulton<sup>a,2</sup>, Alain Goriely<sup>a</sup>, and Régis Chirat<sup>b</sup>

<sup>a</sup>Mathematical Institute, University of Oxford, Oxford, UK; <sup>b</sup>CNRS 5276, Université Lyon 1, 69622 Villeurbanne Cedex, France

This manuscript was compiled on November 17, 2020

1 Brachiopods and mollusks are two shell-bearing phyla that diverged  
2 from a common shell-less ancestor more than 540 million years ago.  
3 Brachiopods and bivalve mollusks have also convergently evolved a  
4 bivalved shell that display an apparently mundane, yet striking fea-  
5 ture from a developmental point of view: when the shell is closed,  
6 the two valve edges meet each other in a commissure that forms a  
7 continuum with no gaps or overlaps despite the fact that each valve,  
8 secreted by two mantle lobes, may present antisymmetric ornamen-  
9 tal patterns of varying regularity and size. Interlocking is maintained  
10 throughout the entirety of development, even when the shell edge  
11 exhibits significant irregularity due to injury or other environmental  
12 influences, which suggests a dynamic physical process of pattern  
13 formation that cannot be genetically specified. Here, we derive a  
14 mathematical framework, based on the physics of shell growth, to  
15 explain how this interlocking pattern is created and regulated by me-  
16 chanical instabilities. By close consideration of the geometry and  
17 mechanics of two lobes of the mantle, constrained both by the rigid  
18 shell that they secrete and by each other, we uncover the mecha-  
19 nistic basis for the interlocking pattern. Our modeling framework  
20 recovers and explains a large diversity of shell forms and highlights  
21 how parametric variations in the growth process result in morpho-  
22 logical variation. Beyond the basic interlocking mechanism, we also  
23 consider the intricate and striking multiscale patterned edge in cer-  
24 tain brachiopods. We show that this pattern can be explained as a  
25 secondary instability that matches morphological trends and data.

morphogenesis | growth | mathematical model | mollusk

1 **B**rachiopods and mollusks are two invertebrate phyla that  
2 possess calcified shells. Evidence derived from molecular  
3 clocks, molecular phylogeny, shell biochemistry and from the  
4 fossil record (1–5) suggest however that they have diverged  
5 from a shell-less common ancestor (Fig. 1). The bivalved  
6 condition of the shell in both brachiopods and bivalve mollusks  
7 is an evolutionary convergence that led several authors to  
8 mistakenly assign brachiopods to mollusks in the early 19th  
9 century (6). One of the most remarkable features of the  
10 shells of brachiopods and bivalves, readily observed but rarely  
11 fully appreciated, is the simple fact that the two valves of  
12 the shell fit together perfectly when the shell is closed, i.e.  
13 throughout the development of the shell the edge of two valves  
14 meet each other in a commissure that forms a continuous  
15 curve with no gaps. At first glance this may not appear  
16 as a surprise, as the two valves comprise two halves of the  
17 same organism. Moreover, it is a trait that brings an easily  
18 understood functional advantage, providing a protective role  
19 against predators and environmental events, and it could be  
20 tempting to conclude that this function alone explains why  
21 both valves closely interlock. However, the function of a trait  
22 does not explain how it is formed during development, which  
23 is the goal of the present work.

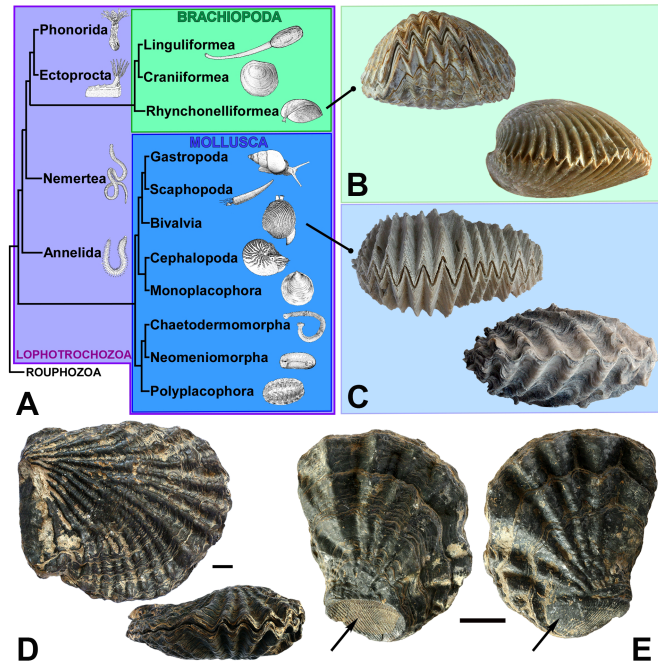


Fig. 1. A. Phylogenetic relationships among brachiopods and mollusks (modified after (5, 7, 8)). B-C Convergent shell commissures in fossil brachiopods (*Septaliphoria orbignyana*; *Kutchirhynchia obsoleta*) and bivalve mollusks (*Rastellum* sp.; *Ctenostreon rugosum*). D. An oyster with irregular interlocking pattern, *Lopha* sp. (Senonian, Algeria). E. Xenomorphic oyster, *Lopha* sp. (Upper Cretaceous, Algeria); the attached valve carries the negative impression of another shell, while the free valve replicates its positive form (as indicated by the arrows).

The two valves of the shell are secreted separately by two lobes of a thin elastic organ, the mantle. Also, the two valves may grow at different rates, have different shapes, and the pattern of shell edge does not exhibit perfect regularity: it may be more or less perturbed, for instance by external factors such as a patterned substrate on which some species live attached, or by environmental events causing shell injuries. Yet, in all cases the interlocking of the two shell edges is tightly maintained. These observations imply that the interlocking pattern emerges as the result of epigenetic interactions modulating the behavior of the secreting mantle during shell development.

Here, we provide a geometric and mechanical explanation for this morphological trait based on a detailed analysis of the shell geometry during growth and the physical interaction of the shell-secreting soft mantle with both the rigid shell edge and the opposing mantle lobe. We demonstrate how an interlocking patterned shell edge emerges naturally as the continuation of a biaxially constrained mechanical instability. We demonstrate how significant morphological variation emerges via parametric variation, and also demonstrate how

44 a secondary instability accounts for the striking multi-scaled  
45 oscillatory patterns found on certain brachiopods.

## 46 1. Background

47 Despite some differences in mode of secretions and anatomy  
48 between bivalves and brachiopods, the shells of both groups are  
49 incrementally secreted at the margin by a thin membranous  
50 elastic organ called the mantle, that secretes first the periostracum,  
51 a thin soft organic layer that serves as a matrix for the  
52 deposition of the calcium carbonate of the shell (9, 10). The  
53 form of the calcified shell may thus be viewed as a spatiotemporal  
54 record of the form taken by the mantle at the shell margin  
55 during development. Though recent studies have begun to  
56 investigate cellular differential growth patterns underlying left-  
57 right asymmetries in gastropods (11) or to identify genetic and  
58 molecular bases of shell biomineralization in both mollusks and  
59 brachiopods (12, 13), the morphogenetic processes underlying  
60 the diversity of shell shapes in both groups remains poorly  
61 known. Theoretical models invoking either reaction-diffusion  
62 chemical systems (14) or nervous activity in the mantle epithelial  
63 cells (15), though successful in capturing the emergence  
64 of pigmentation patterns, do not explain the emergence of  
65 three-dimensional forms. A common default assumption in  
66 developmental biology is that molecular patterning precedes and  
67 triggers three-dimensional morphogenetic processes. While  
68 this assumption might partly motivate recent studies of genetic  
69 and molecular mechanisms involved in shell development, only  
70 two-dimensional pigmentation patterns (that are molecular  
71 in nature) have been shown to map precisely with gene  
72 expression patterns (16). Marginal shell growth in bivalves and  
73 brachiopods takes place when the valves are open, both mantle  
74 lobes being retracted away from the margin of each valve when  
75 the shell is tightly closed. In the case of patterned interlocking  
76 commissures, it is difficult to conceive of genetic and molecular  
77 processes of morphogenetic regulation that would specify that  
78 when the margin of a mantle lobe secretes a patterned edge  
79 on one valve, the same complex processes must regulate the  
80 morphogenesis of the other mantle lobe to generate a perfectly

antisymmetric edge on the other valve, both patterned edges  
closely interlocking when the mantle is retracted and the shell  
is closed. In other words, supposing that molecular patterning  
triggers three-dimensional morphogenetic processes raises the  
question of the nature of the coordinating signal between both  
mantle lobes and how it could be transmitted. Formulated in  
that way, the development of closely interlocking edges, and  
the repeated emergence of similar complex commissures during  
the evolution of two different phyla, are puzzling problems.

A partial answer to this puzzle comes from oysters that  
live attached to a substratum. In these oysters, the surface of  
the attached valve carries the negative impression of the morphology  
of the substratum, while the free valve replicates in positive  
the form of the substratum, a phenomenon known as xenomorphism  
(i.e. ‘having a foreign form’) (Fig.1E). No matter the irregular  
form of the substratum on which the oyster is attached (a stone,  
another shell, an artificial substrate), the edge of the free valve  
closely fits with the edge of the attached valve. As the oyster  
grows bigger, the mantle margin of the attached valve starts to  
turn away from the substratum, and no longer grows attached.  
At this stage, the shell attains what is called its idiomorphic  
form (i.e. ‘having its own form’) (17) and in some species, a  
zigzag-shaped commissure is generated at this stage. Our  
interpretation is that the xenomorphic and idiomorphic parts  
do not differ fundamentally from the point of view of the  
growth processes. In the xenomorphic part, the form taken  
by the mantle margin secreting the attached valve is mechanically  
imposed by the form of the substratum, and this form is  
itself mechanically imposed to the mantle lobe secreting the  
free valve when both mantle lobes are at least temporarily in  
close contact while secreting the slightly opened shell. Once  
the shell no longer grows attached to the substratum, the  
mechanical influence of the substratum is removed and there  
is only a reciprocal mechanical influence between both lobes.  
This reciprocal mechanical influence seems to be a general  
characteristic of the growth of brachiopods and bivalves. For  
example, in the case of traumatic individuals, the non-traumatic  
valve adapts its form and interlocks with the traumatic valve,  
no matter the abnormal form of the shell edge.

Xenomorph-idiomorph transition in oysters and trauma  
mirroring in both bivalves and brachiopods suggest the following  
hypothesis: *interlocking commissures are created by a combination  
of the mechanical constraints acting on each lobe and the  
mechanical influence of the two lobes on each other.* In this  
paper, we develop a theoretical model of shell morphogenesis  
that confirms this hypothesis and extract universal morphogenetic  
rules. We show that the mechanical constraint acting on each  
lobe during growth imposes the geometric orientation of the  
morphological pattern while the reciprocal interaction between  
lobes enforces the antisymmetry of this pattern. Both principles  
are needed for perfect closure and are universal characteristics  
of the growth of brachiopods and bivalves.

## 2. Mathematical model

**A. Base Geometry.** We first describe the general framework  
for the growth of bivalved shells by using the localised growth  
kinematics description of (18, 19). The shell is modeled as  
a surface  $\mathbf{r} = \mathbf{r}(s, t) \in \mathbb{R}^3$ , where  $s$  is a material parameter  
describing location along the shell edge, and  $t$  is a growth “time”

### Significance Statement

A striking feature in bivalved seashells is that the two valves fit together perfectly when closed. This trait has evolved in two phyla from a common shell-less ancestor and has been described for hundreds of years. While its functional advantage is clear, there is no understanding on how this feature is generated. A mathematical model of the shell growth process explains how geometry and mechanics conspire to generate an interlocking pattern. This model provides a physical explanation for a prominent example of convergent evolution. By showing how variations in the mechanism create a wide variety of morphological trends the model provides insight into how biophysical processes, probably modulated by genetic factors, are manifest across scales to produce a predictable pattern.

DEM and RC conceived the study. DEM and AG devised the mathematical model. Computations were performed by DEM. Shells were obtained and photographed by RC. DEM collected data on shell asymmetry. All authors contributed to the writing of the paper.

We have no conflict of interest.

<sup>2</sup>To whom correspondence should be addressed. E-mail: moulton@maths.ox.ac.uk

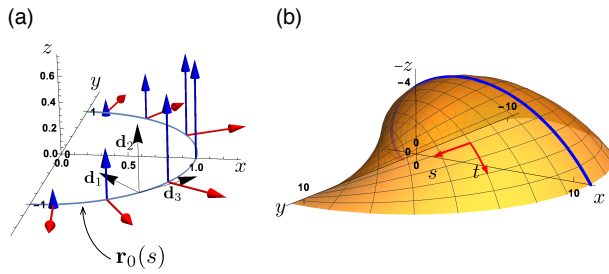


**Fig. 2.** (a) The base geometry for bivalved shells is constructed via a locally defined growth velocity field defined on a base curve  $\mathbf{r}_0(s)$  equipped with orthonormal basis  $\{\mathbf{d}_1, \mathbf{d}_2, \mathbf{d}_3\}$ . The growth consists of dilation (red arrows) and a coiling velocity in the binormal ( $\mathbf{d}_2$ ) direction with linear gradient (blue arrows) and hinge along the  $y$ -axis. (b) The resulting surface for one valve of the bivalve shell, with the  $s$  and  $t$  directions highlighted as well as the longitudinal midline (the curve  $s = 0$ ), which forms a logarithmic spiral.

unknown, ornamentations emerge as the result of mechanical deformations of the secreting mantle margin (20). If the mantle grows at the same rate as the shell edge that it is itself secreting, both mantle and shell are in perfect synchrony and the shell will remain smooth. However, if the mantle margin grows faster, it has an excess of length with respect to the shell edge. This leads to a compressive stress that can induce buckling of the mantle, and the buckled pattern will subsequently be calcified in the next secretion of shell edge. If an excess of length is sustained through development, the deformation pattern will evolve and be amplified. In this way, ornamentation patterns are spatiotemporal records of these continued deformation patterns. This basic mechanism underlies the formation of ornamentation in shells and can be elegantly modeled by treating the mantle edge as a growing elastic beam (the mantle) attached to an evolving foundation (the rigid shell edge). Within this framework, one can explain how basic changes in shell geometry, growth, and mechanical properties produce a diverse morphology of ornamentation patterns (21–24). Here, we use the same modeling framework adapted to the growth constraints in bivalved shells.

**C. Ornamentation orientation.** In our model the shell is obtained as the superposition of the morphological pattern of the buckled mantle on the smooth geometric surface generated via the growth velocity field. Antimarginal ornamentation is generally understood as a morphological pattern in the plane orthogonal to the shell margin, i.e. in the plane which has normal vector pointing tangent to the direction of shell growth (the plane with normal vector  $\dot{\mathbf{r}}$  in the geometric description outlined above). However, close inspection of bivalved seashells shows that ornamentations typically do not form in the orthogonal plane and a natural problem is to determine the orientation of the ornamentation plane. Fig. 3(a) illustrates an oscillation pattern in the antimarginal plane as well the same pattern in a rotated plane.

The solution to this problem is the first key component that produces interlocking. The length of shell in the growth direction (i.e. arclength in the  $t$ -direction for fixed material point  $s$ ) is determined by the rate of secretion. For neighboring material points the rate of secretion and thus arclength in the smooth shell are nearly identical. Once the mantle (and thus the shell edge) deforms, these arclengths may differ, depending on the plane in which the deformed pattern appears, and this will produce a moment of force about the shell edge (the  $\mathbf{d}_3$  direction) that serves to rotate the plane. The idea is illustrated in Fig. 3(b)-(c). Fig. 3(b) shows a portion of a base shell (yellow), and the same shell with a half-mode oscillation pattern imposed on top (red), with the pattern appearing in the antimarginal plane.\* Once the mantle deforms, however, the arclengths are no longer equal: the arclength at the point which has deformed “up” is longer than the arclength at the point which has deformed “down”, i.e.  $l_u > l_d$  as pictured. This difference creates a differential strain in the generative zone, the deformable region that connects the mantle to the already calcified portion of the shell, which induces a moment of force acting on the mantle that rotates the plane of ornamentation. In Fig. 3(c), the same mode of deformation is shown in a rotated plane where the arclength at the “up” and “down”

\* Locally, a small section of shell can be approximated as a cylinder with logarithmic spiral shape and with equal arclength at neighboring points prior to mantle deformation, hence for visual simplicity here we plot portions of the shells as being cylindrical.

parameter which need not correspond to actual time but which increases through development. The shell is constructed by defining an initial curve  $\mathbf{r}(s, 0) = (x_0(s), y_0(s), 0)$  (where  $s$  is the arclength) and a growth velocity field  $\mathbf{q}(s, t)$  representing the rate of shell secretion such that  $\dot{\mathbf{r}} = \mathbf{q}$ , (overdot represents time derivative). In the case of bivalved shells, the field  $\mathbf{q}$  requires only two components: a dilation rate, denoted  $c$ , which describes the rate of expansion of the aperture, and a coiling rate, denoted  $b$ , which is equivalent to the gradient in growth in the binormal direction and dictates how tightly coiled the shell is (see Fig 2). However, since we are only interested in the shape we can set the dilation rate to  $c = 1$  without loss of generality, as it is only the ratio of dilation to expansion that is relevant in the shell form.

The key to this description is to express the velocity field in a local orthonormal basis  $\{\mathbf{d}_1, \mathbf{d}_2, \mathbf{d}_3\}$  attached to each point of the shell edge. Here, we choose  $\mathbf{d}_3$  to be tangent to the shell edge, i.e.  $\mathbf{r}'(s, t) = \lambda(t)\mathbf{d}_3$ , where prime denotes derivative with  $s$  and  $\lambda$  is a scale parameter characterizing the degree of total dilation from the base curve. Defining  $\mathbf{d}_2$  to align with the binormal direction, coiling is generated through a binormal growth velocity component  $q_2 = bx_0(s)$ ; i.e. shell coiling requires a linear growth gradient along an axis (taken without loss of generality to be the initial  $x$ -axis). Bivalves also require a hinge; in this formulation the hinge is the  $y$ -axis, where  $x_0 = 0$  and thus  $q_2 = 0$ ; see Fig. 2 and further geometric details in Supplementary Information (SI) Appendix Section 1. The benefit of this approach is that the base shape of the shell emerges through a single geometric growth parameter, the coiling rate  $b$  that can be related to a self-similar process of secretion of shell material and growth of the mantle. We do not assume a symmetry between the two valves, i.e. the coiling rates for the two halves may be different as seen in brachiopods (see Section 3C). Nevertheless, due to fixed dilation ( $c = 1$  for both valves), if both halves have the same initial curve then the two valves (of the smooth shell) will always meet perfectly in the  $x$ - $y$  plane when the base shell is closed.

**B. Mechanical basis of ornamentation.** In bivalves and brachiopods, three-dimensional ornamentations typically consist of an oscillation pattern of the shell edge that is termed *antimarginal ornamentation*. The basic premise for our investigation is that while the developmental processes underlying the variations of base geometry of the shell remain largely

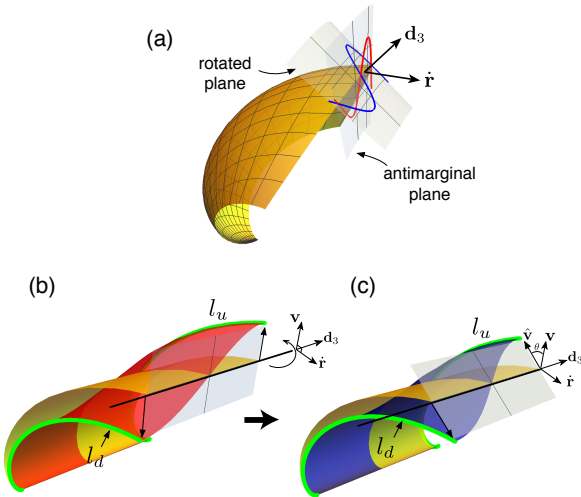


**Fig. 3.** (a) The difference between pattern imposed in the antimarginal plane, with normal vector  $\hat{r}$ , and a rotation of this plane about the  $\mathbf{d}_3$  direction. In (b), an oscillatory pattern in the antimarginal plane creates an unbalanced strain in the generative zone, as the arclength at the valleys is less than at the peaks. In the schematic, the green curve  $l_d$  has shorter length  $l_u$ . This strain creates locally a moment around the  $\mathbf{d}_3$  axis. (c) This moment is balanced by rotating the plane of ornamentation until the arclengths are made equal and the strain balanced.

coincide, i.e. the sinusoidal curves are in phase, significant gaps and overlaps appear so that the valves do not interlock. Fig. 4(b) shows the same shell, but with a rotation of the plane of ornamentation. Here, a perfect interlocking is attained. Intuitively, the reason that the two valves can interlock is that the rotation imposed by generative zone strain causes both patterns to develop *in the same plane*.

The argument and calculation in Section C provides a geometric condition for the local orientation of the plane of each valve, though it is to be noted that this condition does not take into account the presence of the other valve. However, when both valves are rotated to meet in the  $x$ - $y$  plane, Rule 1 is satisfied. Indeed, the plane of ornamentation for the shell in Fig. 4(b) was computed according to the calculation described above. In fact we find that this is a generic feature: for a bivalved shell growing according to the rules outlined above, and with plane of ornamentation defined by the balance of moments Eq. (1), the planes of ornamentation of each valve almost perfectly coincide at all points along the shell edge and at all times throughout development (see Section 2 of SM).

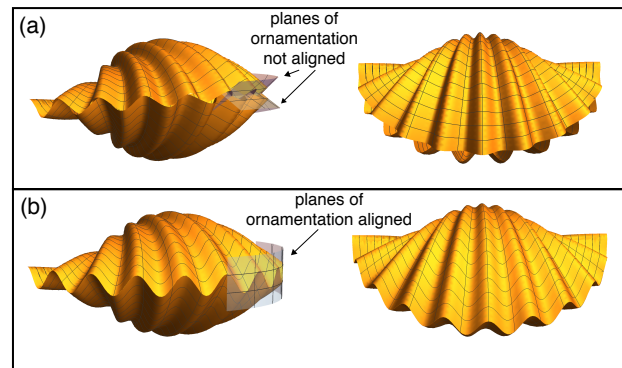


**Fig. 4.** The first rule of interlocking: At the shell level rotating the ornamentation plane is important for interlocking. A non-rotated plane of ornamentation (a) leads to a misalignment of the ornamentation patterns and thus gaps and overlaps appear when the two valves are closed. With rotation (b), opposing planes agree and a perfect interlocking is attained.

### E. Rule 2: In-phase synchrony of ornamentation pattern.

While the coplanarity of ornamentation planes ensures that the two ornamentation patterns will appear in the same plane, it does not in itself guarantee that the two valves will interlock. For this to occur, we also require Rule 2 of interlocking: *the ornamentation patterns must coincide in phase*. We now show that this synchrony is born out of the mechanical interaction of the two opposing mantle lobes.

Following (22, 23), we treat each mantle edge as a morphoelastic rod (25) attached elastically via the generative zone to a foundation, the rigid calcified shell (see details in SI Appendix Section 3). The two mantle edges interact with each other when in contact through a repulsive interaction force ensuring that the two mantles cannot interpenetrate.

Since the two valves are meeting at a common plane with equivalent length of shell edge, and assuming that the mantle tissue of each valve has the same mechanical properties, given an excess of length that induces a mechanical pattern, the preferred buckling mode for each respective valve will be the same, if considered in isolation. The question then is what form the buckled pattern will take when the two mantle edges

points are equal,  $l_u = l_d$ , so that the differential strain and thus the moment vanishes.

The precise degree of rotation that balances the strain depends on the stage of development, the material point along the shell edge, and the growth parameters for the base shell. In particular it is worth noting that the steeper the angle of commissure, which occurs with increased coiling rate  $b$ , the more rotation is needed. This is intuitive, if one considers that for a perfectly flat shell there is a perfect symmetry between “up” and “down” deformations, and thus no rotation is needed. Mathematically, points on the upper and lower side of the pattern are located at  $\mathbf{r}_{\text{up,down}} = \mathbf{r} \pm \epsilon \lambda \hat{\mathbf{v}}$  where  $\epsilon$  is the amplitude of deflection of the mantle, the factor  $\lambda$  accounts for the scaling of the buckling pattern’s amplitude, and  $\hat{\mathbf{v}}$  is a unit vector to be determined that describes the orientation of the pattern such that the ornamentation appears in the  $\mathbf{d}_3$ - $\hat{\mathbf{v}}$  plane (details in SI Appendix Section 2). Then the balance of moment can be written as a geometric condition

$$\hat{\mathbf{r}} \cdot (\lambda \hat{\mathbf{v}} + \lambda \hat{\mathbf{v}}) = 0. \quad [1]$$

This is a nonlinear differential equation satisfied by the rotation angle, which will depend on both the material point  $s$  and the development time  $t$ .

**D. Rule 1: Coplanarity of ornamentation planes.** For perfect interlocking to occur, the pattern on each individual valve must locally occur in the same plane when the valve is closed. We state this as the first rule of interlocking: *the ornamentation planes of the two opposing valves must be aligned at all points when the valves are closed*. This geometric rule is illustrated in Fig. 4, in which we superimpose a sinusoidal ornamentation on a bivalve. In Fig. 4(a) the ornamentation is truly antimarginal, i.e. there is no rotation of the plane of ornamentation. In this case, even though the pattern on the two valves was chosen to

are not in isolation, but interacting with each other. The problem is greatly simplified by the first rule: since the two planes of ornamentation are locally aligned, we can consider the buckling problem in a single surface. Further assuming that the curvature of the mantle along the edge is small, we ‘unwrap’ the common ornamentation surface and consider a planar problem. For a given excess of length due to mantle growth, we compute the possible modes of deformation for the two mantles parametrically given by  $(x_i(s), y_i(s))$ ,  $i = 1, 2$ , in the  $x$ - $y$  ornamentation plane (SI Appendix Section 3). Once these are found, we consider the total mechanical energy of the system, given by the sum of bending and foundation energies on each side and the interaction energy between the two:

$$\mathcal{E} = \mathcal{E}_{\text{bend}}^{(1)} + \mathcal{E}_{\text{bend}}^{(2)} + \mathcal{E}_{\text{found}}^{(1)} + \mathcal{E}_{\text{found}}^{(2)} + \mathcal{E}_{\text{interaction}} \quad [2]$$

where

$$\mathcal{E}_{\text{bend}}^{(i)} = \frac{1}{2} m_i(s)^2, \quad \mathcal{E}_{\text{found}}^{(i)} = \frac{k}{2} (y_i(s) - (-1)^i \delta)^2. \quad [3]$$

Here  $\delta$  denotes the half-width of each mantle,  $m_i$  is the resultant moment acting on the growing mantle, and  $k$  describes the strength of the foundation. The interaction between both mantles is

$$\mathcal{E}_{\text{interaction}} = f((y_1 - y_2) - 2\delta)^{-2}, \quad [4]$$

where  $f$  is a constant that characterises the strength of the repulsive interaction. We compare the energy in two distinct configurations: one in which the opposing mantle edges are ‘in phase’, and one in which they are ‘out of phase’. These configurations are obtained by first computing the preferred buckling shape of a mantle in isolation. The buckling forms a bifurcation from the trivial straight solution with two solution branches of equal energy that are mirror images of each other. Taking both mantles from the same branch forms the ‘in-phase’ solution while taking them from opposing branches forms the ‘out-of-phase’ solution. We then compute the energy in the system as a function of mantle growth. The energies are plotted in Fig. 5(c), which shows that the energy in the ‘out of phase’ pattern is significantly higher than the ‘in phase’ energy. For comparison, we compute the energy of the two mantles in the absence of interaction (dashed line), which forms a lower bound on the total energy.

The complete shell with the energy minimising buckling pattern imposed is plotted in Fig. 5(b). Physically, the ‘in phase’ pattern has lower energy because a large deformation is needed to maintain geometric compatibility in the ‘out of phase’ case, and the contact energy is also much higher. The significant difference in energy between ‘in phase’ and ‘out of phase’ deformation modes (almost double at the point of only 3% growth extension) and the close proximity of ‘in-phase’ energy with the lower bound ‘no interaction’ energy, suggests that the ‘in phase’ solution is a global minimizer and the preferred configuration. We conclude that the mechanical interaction of the mantles provides the mechanism for Rule 2.

### 3. Morphological trends

**A. Growth, accretion, and secretion.** The formation of a shell involves three distinct but closely related activities: growth of the mantle, secretion of new shell material by the mantle, and accretion of the shell. The distinction between secretion

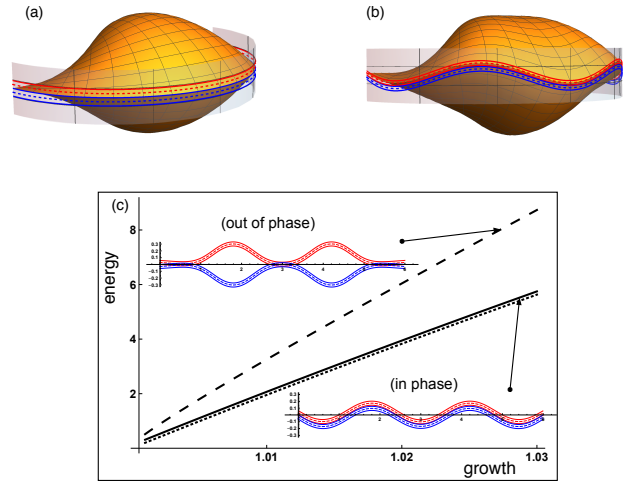


**Fig. 5.** The ornamentation pattern emerges as a mechanical instability due to excess growth of the shell secreting mantle and periostracum. In the model, the mantle edge (a) is ‘unwrapped’ to compute the 2D pattern which is then imposed back on the shell in the plane of ornamentation (b). In (c), an energy comparison demonstrates that the ‘in phase’ pattern with interlocking edges is energetically favorable and nearly identical to the energy without interaction between the mantles (dotted curve in (c)).

and accretion is subtle, but if we define accretion as increase of shell length in the growth direction, then it becomes clear that it is possible for shell material to be secreted without actually contributing to accretion, e.g. by thickening the shell as empirical evidence shows in many seashells. To explain the distinction between observed morphologies requires considering the interplay between these activities.

We first consider the link between mantle growth and secretion rate. By mantle growth we refer specifically to longitudinal growth along the mantle edge – the growth that produces the excess of length that drives mantle buckling and thus generates the patterned shell edge. The rate of amplification of the buckling pattern is governed by the rate of mantle growth. Here we make the simple assumption that the mantle growth rate is proportional to the secretion rate  $b$ . In this way, a shell with higher coiling rate (larger  $b$ ) will have a higher ornamentation amplitude compared to a shell with lower coiling rate. In particular, the linking of growth with secretion provides a simple mechanism for zigzag commissures (see Fig. 1C), which tend to appear in shells with very steep angle of commissure (high coiling rate): these may be seen as an extreme form of a (smooth) buckling pattern but with a very small wavelength combined with a high amplitude, the latter arising due to high secretion rate.

**B. A 2D morphospace.** In this construction, there are only two main parameters governing the shell morphology: the coiling rate  $b$ , and a single mechanical parameter  $k$  (see SI Appendix Section 3), which governs the mode of buckling and hence the wavelength of the interlocking ornamentation pattern<sup>†</sup>.

In Fig. 6 we illustrate the range of shell morphologies as a 2D morphospace formed by the parameters  $k$  and  $b$ . A low value of  $k$  results in a long wavelength pattern, and vice versa, while a low coiling rate produces a shallow shell, with high coiling

<sup>†</sup> The cross-sectional shape is another degree of freedom, and indeed our approach may be applied to any cross-sectional shape, but we have restricted to a semi-circle here, as this provides the simplest form and is a good model for most bivalved shells.

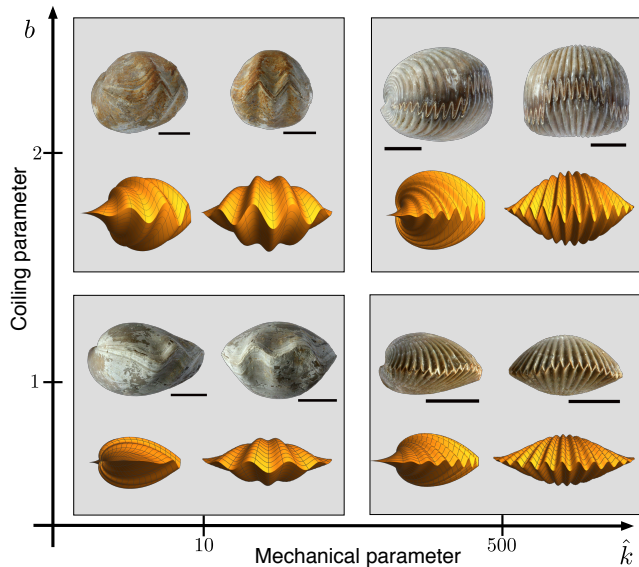


**Fig. 6.** Morphology variety for (symmetric) interlocking bivalved shells and sample shells illustrating the diversity of form. The simulated shells correspond to the 4 different combinations of a low ( $b = 1$ ) and high ( $b = 2$ ) coiling rate and small ( $k = 10$ ) and large ( $k = 500$ ) mechanical stiffness. The computational procedure is outlined in SI Appendix Section 4.

that one valve, say valve 1, has a higher secretion rate than the other one, say valve 2. The corresponding mismatch in mantle growth means that mantle 1 will have a greater (unstressed) reference length, but is under the same geometric constraints as mantle 2. This mismatch induces a mechanical stress in the mantle tissue which is relieved by a secondary buckling instability of the entire mantle/periostacum tissue<sup>§</sup>.

**C.1. Adaptive accretion.** As a first test of the model, we check that interlocking is maintained within the framework we have developed. In the base case, before any deformation, the coiling rates are constant for each valve, and the two valve edges meet at the same mid-plane when the valves are closed. Once a large-scale deformation occurs, the valve edges no longer meet in a single plane (the  $x - y$  plane as in the base case). Some material points along the edge will have moved in one direction (to  $z > 0$  say) while other points will have moved the other direction ( $z < 0$ ). However, the rotation of each valve about the hinge – increased rotation is needed to accommodate increased material – is a *global* property. Thus, the geometrical constraint of the presence of the opposing valve *locally* changes along the shell edge. The local accretion rate, i.e. local coiling rate, must change in response. By analysing the coiling geometry with such a deformation imposed, we show in SI Appendix Section 5 that the coiling naturally adapts such that the two shell edges still perfectly coincide, though no longer in a single plane.

The next step is to reintroduce the small-scale pattern by the same process as before: a generative zone strain is induced by the difference in arclength at the valleys compared to the peaks of the small-scale pattern, and thus the plane of ornamentation is defined such that the arclength is equal at the peaks and valleys. The corresponding nonlinear ODE is then solved for the tilt of mantle that defines the local plane of ornamentation (details in SI Appendix Section 5A). The net result is that the plane of ornamentation rotates non-uniformly at each point along the shell edge compared to the base case, but the orientations still coincide locally between the two valves. Thus Rule 1 is satisfied even in the presence of asymmetry.

**C.2. Synchrony of ornamentation with asymmetry.** The conceptual idea of Rule 2 is as before: for interlocking to occur the ornamentation patterns must be antisymmetric, a synchrony we expect to be maintained by the mutual interaction of the mantles. However, the situation is more complicated by the difference in mantle growth rates and requires an extension of the previous mechanical model for two mantles geometrically constrained by each other with the additional assumption that they are growing at unequal rates (see SI Appendix Section 6).

We find that for moderate asymmetry, the interaction of the mantles is sufficient to enforce synchrony of the pattern. However, as further elucidated in SI Appendix Section 6, for larger asymmetry the mantles eventually separate due to a divergence in their reference lengths. A bio-mechanical coupling would be necessary in such cases.

**C.3. Asymmetry patterns.** We confirm the prediction of our model against basic morphological trends observed in shells

rate producing a steeper shell and more amplified pattern. For comparison, we include four representative shells matching the basic characteristics of each corner of the morphospace. Since by construction these shells satisfy both rules of interlocking, the interlocking pattern is perfectly formed.

**C. Asymmetry and secondary ornamentation.** An intriguing feature of our findings is that interlocking does not require symmetry between the two valves (consider: your two hands clasp together very nicely, but they also grow as almost perfect mirror images). Indeed, in many shells, notably in brachiopods, the two valves have markedly different coiling rates. In our model, Rule 1 is accomplished by a rotation of the generative zone that does not rely on the physical interaction of the opposing valve, thus the two base valves need not be mirror images of each other for the planes of ornamentation to align. And once the planes align, Rule 2 for antisymmetry of the pattern is accomplished by the mechanical interaction of the two mantles.

However, by linking mantle growth to secretion rate, an asymmetry in coiling implies also an asymmetry in mantle growth. Therefore, we can put our modeling framework to the test by studying the ornamentation morphology of shells with asymmetric coiling. In particular, we are motivated by a striking feature found in some brachiopod shells, as shown in Fig. 7. These shells exhibit a secondary, long wavelength pattern, on top of which a small wavelength primary pattern can be found<sup>‡</sup>. Both the long and short wavelength patterns vary significantly between species and specimens, yet remarkably, perfect interlocking is maintained in all cases.

To study the impact of asymmetry in the model we suppose

<sup>‡</sup>We term the long wavelength pattern as secondary, as this pattern only ever appears later in development, while the small scale ornamentation appears early and has the same characteristics as the ornamentations we have described thus far in this paper.

<sup>§</sup>In this view, the small scale pattern is primarily focussed at the thin periostacum while the much thicker mantle remains effectively flat; see SI Appendix Section 5 and SI Appendix Fig. 2.

with the secondary pattern. In Brachiopods the two valves cover the dorsal and ventral sides of the animal. Prior to the large-scale deformation, the dorsal side has the higher coiling rate (when there is asymmetry present). Once the large scale pattern appears, the following characteristics are observed:

- (i) The large wavelength pattern appears either as an “even mode” or an “odd mode” (see Fig. 7(c)).
- (ii) There is a positive correlation between the degree of dorso-ventral asymmetry and the size of the large-scale pattern.

Observation (i) is clearly compatible with a mechanical instability, for which different buckling modes will be triggered based on geometric and mechanical parameters. For odd modes, there is no lateral preference, i.e. right and left “handed” shells with an odd mode always occur in roughly the same numbers in populations (26) and in the 29 known cases of plant and animal displaying random direction of bilateral asymmetry, the direction of asymmetry almost always lacks a genetic basis (27). A mechanical origin is consistent with this trend, as there is no lateral preference in the case of an odd mode buckling, by symmetry of the geometry. With even modes, on the other hand, the middle point of the shell edge *always* deforms towards the dorsal valve. This requires a bias in the buckling direction that only impacts even modes; a plausible mechanism based on the already present coiling asymmetry is described in SI Appendix Section 6.

Observation (ii) is also consistent with a mechanical process, as an increase in dorso-ventral asymmetry would imply an increase in mechanical stress, which would lead to earlier buckling and an increased amplitude relative to shell size. To quantify this trend, we have studied a sample of 59 brachiopods from different species. For each shell, we extract dorso-ventral asymmetry by fitting a logarithmic spiral to a side profile, and amplitude of the large pattern by fitting a sinusoid to a front view, as shown in Fig. 7(a). Amplitude is plotted against asymmetry in Fig. 7(b), showing a strong correlation: we compute a Spearman’s rank correlation coefficient of 0.67, and a p-Value less than 0.0001. The extracted data, as well as an image of every shell sampled with curves overlaid, is available in SI Appendix Section 7. From the mechanical model (SI Appendix Section 6) we extract the equivalent measures by taking the difference in asymmetry to correspond to the difference in mantle growth rates, computing the bifurcation curves following buckling and extracting amplitude relative to length for several different measures of asymmetry. These appear as the orange squares in Fig. 7(b), demonstrating that the patterns and trends predicted by the model are consistent with the observed morphological trends.

Moreover, the morphological features are well captured by the model. To illustrate, the computed buckled shape at the two marked simulated points in Fig. 7(b) was fed into the full shell model, with small pattern taken as output of the small-scale mechanical model and plane of ornamentation computed with adapted coiling in combination with base shell geometry; all model components combined to produce the simulated shells appearing in Fig. 7(b), which in both cases exhibit a perfect interlocking.

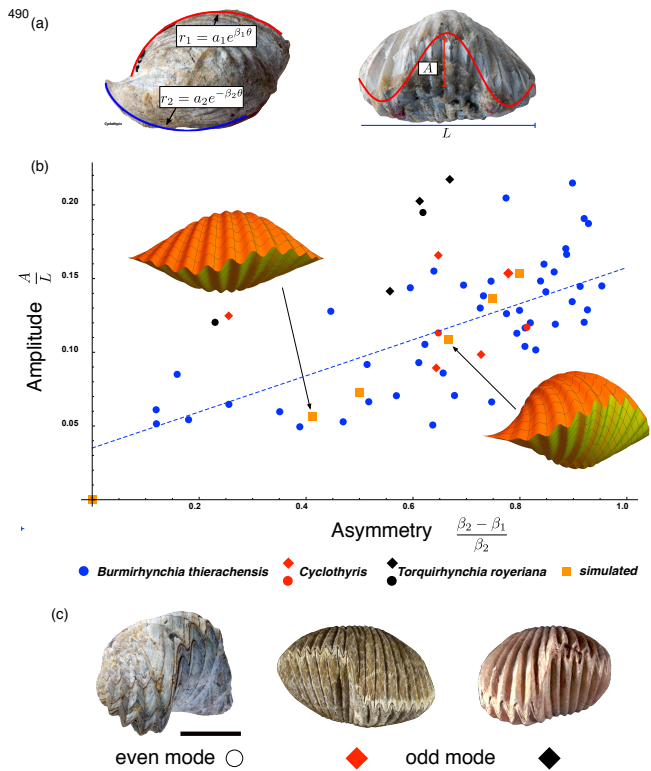


**Fig. 7.** Asymmetry and large-scale pattern in brachiopods. (a) For each shell we extract both *asymmetry* measure via difference in coiling rates and relative *amplitude* of the large pattern. (b) These data are collected on a set of shells displaying the large scale pattern: *Burmirhynchia thierachensis* (blue), *Cyclothyris* (red), and *Torquirhynchia royeriana* (black). Shells displaying odd mode are marked with a diamond symbol. A linear regression is plotted as the dashed line. The orange squares are produced via a two-beam mechanical model, and complete shells are simulated at the marked points. (The hollow point at the origin is not simulated; by construction zero asymmetry has zero amplitude.) (c) Large wavelength patterns in Brachiopods appear both as an “even mode” deformation (left: *Septaliphoria orbignyana*) and “odd mode” (middle: *Cyclothyris* sp. and right: *Torquirhynchia royeriana*). In the latter, there is no lateral preference.

#### 4. Discussion

In this paper we have shown the key role of mechanics in forming common features of shell sculpture in interlocking bivalved shells. Ornamentation appears as a mechanical instability arising due to a simple developmental change – growth of the mantle outpacing expansion of the aperture – while at the same time shell interlocking is maintained by mechanical forces without requiring specific genetic processes. This biophysical explanation of developmental origins provides a much-needed complementary view to functional considerations. Indeed, during the 20th century most aspects of brachiopods and mollusk shells morphologies have been interpreted within the functional perspective of the neo-Darwinian synthesis. According to this view one may explain how a trait has come into being and has evolved by appealing to its function alone. For instance, Rudwick (28) proposed that zigzag-shaped commissures have evolved as filtering grids to prevent the entry of harmful particles above a certain size in brachiopods and bivalves that feed by filtering tiny food particles from seawater, and concluded that this function explains the presence of this trait and the intrinsic probability that zigzags evolved many times indepen-

dently in these organisms, an interpretation that has since remained unquestioned (29, 30). However, the promotion of traits by natural selection is logically distinct from the mechanisms that generate them during development. While some of the possible functional advantages of interlocking structures are clear, an explanation of the repeated emergence of similar characters in distantly related lineages requires an understanding of the development of these characters that might induce a reproductive bias (i.e. natural selection).

Our study shows that a part of the morphological diversity and evolution of these groups of invertebrates may be understood in light of both the mechanical interactions of the mantle with the rigid shell edge, and the reciprocal mechanical influence that both mantle lobes have on each other during shell secretion. Our conclusion is that brachiopods and bivalves have managed to secrete interlocking shells simply as a consequence of a biaxially constrained mechanical instability of the secreting mantle. It is therefore not surprising that the same patterns of interlocking structures have evolved repeatedly among brachiopods and bivalves, an evolutionary trend which is a predictable outcome of the physics of the growth process. It is also worth noting that we have restricted our study to self-similar shell growth (prior to emergence of any large-scale pattern) and with small-scale patterns appearing at right angles to the shell margin. While it is a suitable assumption for most bivalves and brachiopods, there are species that deviate from self-similarity or with ribs appearing oblique to the shell margin. In such shells interlocking is consistently maintained, suggesting that the process we propose is robust with respect to these perturbations as well. Accordingly, we hypothesize that mechanical forces also play the same role in these systems. However, to model these forces explicitly would require introducing an additional torsional component in the generative zone<sup>†</sup> and/or deviating from the self-similar growth that we have utilized in our geometric construction. While such steps are certainly feasible, and conceptually all of the same ideas outlined in our paper would still apply, modelling such cases would introduce additional computational complexity and is left as future work.

There are other striking examples in nature of organisms with matching of body parts, such as the closed mouth of the snapdragon flower (28, 29), the interacting gears of the planthopper insect *Issus* (30), or dental occlusion in vertebrates (31). The role of mechanics in the morphogenesis of such structures could be the subject of fruitful future inquiries. Among mollusks, the hinge in bivalves is also formed by a series of interlocking teeth and sockets on the dorsal, inner surface of the shell. In this case too, the hinge teeth are secreted by two lobes of the mantle which are retracted from the hinge line when the shell is tightly closed and when teeth and sockets interlock in each other. The morphology of these hinge teeth (e.g. taxodont, heterodont, schizodont...) have traditionally provided the basis of bivalve classifications, but recent molecular phylogenies (32) show that these characters do not always bear a coherent phylogenetic signal, which could be explained by the fact that ahistorical physical processes play an important role in their development.

The fact that physical processes are key in shell morphogenesis does not imply that genetic and molecular processes are

<sup>†</sup>In terms of the plane of ornamentation, our model considers a rotation about the tangent  $d_3$  direction; an oblique pattern could be produced by also rotating about the  $d_2$  direction, which would create a 'slant' to the antimarginal ornamentation

irrelevant. For example, both the amplitude and wavelength of ornamentation may vary considerably among oyster species, possibly because of species-specific combinatorial variations in control parameters such as commarginal growth rate or stiffness of the mantle. Given that these parameters may be genetically modulated, our approach might open the door to future studies aiming at understanding how biochemical and biophysical processes across scales could conspire to regulate the development and variations of morphologies among different species. The interplay between predictable patterns and unpredictability of specific outcomes in large part defines biological evolution (33). Cells, tissues, and organs satisfy the same laws of physics as non-living matter, and in focusing on the noncontingent and predictable rules that physical processes introduce in development and in the trajectories that are open to morphological evolution, we shift the focus from the Darwinian perspective of "the survival of the fittest", to a more predictive one of "the making of the likeliest".

While buckling and wrinkling instabilities have long been viewed as only detrimental in engineering, an increasing number of studies, often inspired by biology, have shown the potential contribution of this physical phenomenon to smart applications (34). Interlocking structures are ubiquitous in man-made structures where they serve as physical connections between constitutive parts in such diverse areas as building or biomedical engineering, and their presence in nature is a source of inspiration for biomimetic engineering (35). Our study shows that brachiopods and bivalves have made good use of mechanical instabilities to secrete their interlocking shell since about 540 million years; in this light perhaps the growth of these invertebrates could be inspirational in biomimetic research for the development of self-made interlocking structures at many scales.

## Data availability

All materials, methods, and data needed to evaluate the conclusions are present in the main article and/or SI Appendix.

1. Kouchinsky A, et al. (2012) Chronology of early cambrian biomineralization. *Geological Magazine* 149(2):221–251.
2. Peterson KJ, Cotton JA, Gehling JG, Pisani D (2008) The ediacaran emergence of bilaterians: congruence between the genetic and the geological fossil records. *Philosophical Transactions of the Royal Society B: Biological Sciences* 363(1496):1435–1443.
3. Luo YJ, et al. (2015) The lingula genome provides insights into brachiopod evolution and the origin of phosphate biomineralization. *Nature communications* 6:8301.
4. Isowa Y, et al. (2015) Proteome analysis of shell matrix proteins in the brachiopod *laqueus rubellus*. *Proteome science* 13(1):21.
5. Laumer CE, et al. (2015) Spiralian phylogeny informs the evolution of microscopic lineages. *Current Biology* 25(15):2000–2006.
6. Williams A, Carlson SJ, Brunton CHC, Holmer LE, Popov L (1996) A supra-ordinal classification of the brachiopoda. *Philosophical Transactions of the Royal Society of London. Series B: Biological Sciences* 351(1344):1171–1193.
7. Kocot KM, et al. (2011) Phylogenomics reveals deep molluscan relationships. *Nature* 477(7365):452.
8. Carlson SJ (2016) The evolution of brachiopoda. *Annual Review of Earth and Planetary Sciences* 44:409–438.
9. Simkiss KW, Wilbur K (1989) K.. 1989. biomineralization. *Cell Biology and Mineral Deposition, Academic Press, San Diego*.
10. Roda MS, et al. (2019) Calcite fibre formation in modern brachiopod shells. *Scientific reports* 9(1):598.
11. Johnson AB, Fogel NS, Lambert JD (2019) Growth and morphogenesis of the gastropod shell. *Proceedings of the National Academy of Sciences* 116(14):6878–6883.
12. Jackson DJ, Wörheide G, Degnan BM (2007) Dynamic expression of ancient and novel molluscan shell genes during ecological transitions. *BMC evolutionary biology* 7(1):160.
13. Jackson DJ, et al. (2015) The magellania venosa biomineralizing proteome: a window into brachiopod shell evolution. *Genome biology and evolution* 7(5):1349–1362.
14. Meinhardt H (1995) *The algorithmic beauty of sea shells*. (Springer-Verlag).
15. Boettiger A, Ermentrout B, Oster G (2009) The neural origins of shell structure and pattern in aquatic mollusks. *Proceedings of the National Academy of Sciences* pp. pnaas–0810311106.
16. Jackson DJ, et al. (2006) A rapidly evolving secretome builds and patterns a sea shell. *BMC biology* 4(1):40.

- 697 17. Stenzel HB (1971) Oysters. *Treatise on Invertebrate Paleontology, Part N, Bivalvia* 3 pp. N953–N1224.
- 698 18. Moulton DE, Goriely A (2014) Surface growth kinematics via local curve evolution. *Journal of mathematical biology* 68(1-2):81–108.
- 699 19. Goriely A (2017) *The Mathematics and Mechanics of Biological Growth*. (Springer Verlag, New York).
- 700 20. Moulton DE, Goriely A, Chirat R (2012) Mechanical growth and morphogenesis of seashells. *Journal of theoretical biology* 311:69–79.
- 701 21. Erlich A, Howell R, Goriely A, Chirat R, Moulton DE (2018) Mechanical feedback in seashell growth and form. *The ANZIAM Journal* 59(04):581–606.
- 702 22. Chirat R, Moulton DE, Goriely A (2013) Mechanical basis of morphogenesis and convergent evolution of spiny seashells. *Proceedings of the National Academy of Sciences of the United States of America* 110(15):6015–6020.
- 703 23. Moulton DE, Goriely A, Chirat R (2015) The morpho-mechanical basis of ammonite form. *Journal of theoretical biology* 364(C):220–230.
- 704 24. Erlich A, Moulton DE, Goriely A, Chirat R (2016) Morphomechanics and developmental constraints in the evolution of ammonites shell form. *Journal of Experimental Zoology Part B: Molecular and Developmental Evolution* 326(7):437–450.
- 705 25. Moulton DE, Lessinnes T, Goriely A (2012) Morphoelastic rods Part 1: A single growing elastic rod. *Journal of the Mechanics and Physics of Solids* 61(2):398–427.
- 706 26. Fürsich FT, Palmer T (1984) Commissural asymmetry in brachiopods. *Lethaia* 17(4):251–265.
- 707 27. Palmer AR (2004) Symmetry breaking and the evolution of development. *Science* 306(5697):828–833.
- 708 28. Cui ML, Copsey L, Green AA, Bangham JA, Coen E (2010) Quantitative control of organ shape by combinatorial gene activity. *PLoS biology* 8(11):e1000538.
- 709 29. Green AA, Kennaway JR, Hanna AI, Bangham JA, Coen E (2010) Genetic control of organ shape and tissue polarity. *PLoS biology* 8(11):e1000537.
- 710 30. Burrows M, Sutton G (2013) Interacting gears synchronize propulsive leg movements in a jumping insect. *science* 341(6151):1254–1256.
- 711 31. Calamari ZT, Hu JKH, Klein OD (2018) Tissue mechanical forces and evolutionary developmental changes act through space and time to shape tooth morphology and function. *BioEssays* 40(12):1800140.
- 712 32. Plazzi F, Ceregato A, Taviani M, Passamonti M (2011) A molecular phylogeny of bivalve mollusks: ancient radiations and divergences as revealed by mitochondrial genes. *PLoS One* 6(11):e27147.
- 713 33. Koonin EV (2011) *The logic of chance: the nature and origin of biological evolution*. (FT press).
- 714 34. Hu N, Burgueño R (2015) Buckling-induced smart applications: recent advances and trends. *Smart Materials and Structures* 24(6):063001.
- 715 35. Zhang Y, Yao H, Ortiz C, Xu J, Dao M (2012) Bio-inspired interfacial strengthening strategy through geometrically interlocking designs. *journal of the mechanical behavior of biomedical materials* 15:70–77.
- 716
- 717
- 718
- 719
- 720
- 721
- 722
- 723
- 724
- 725
- 726
- 727
- 728
- 729
- 730
- 731
- 732
- 733
- 734
- 735
- 736
- 737
- 738